Analysis of Optical Waveguides With Multilayer Dielectric Coatings Using Plane Wave Expansion

Thach Giang Nguyen and Arnan Mitchell, *Member, IEEE*

***Abstract*—A numerical analysis of optical waveguides with multilayer dielectric coatings is presented. The simulation is based on the plane wave expansion method, taking into account the exact guided mode profile of the waveguide. The method is free from any assumption about the homogeneity of the waveguide. The power reflectivity is calculated for both antireflection coatings and high-reflection coatings. The accuracy of the model is verified by comparing with the exact results and other simulation methods. The speed and accuracy of the plane wave expansion method make it suitable for direct numerical optimization. The method can also be used as an analytic tool to analyze the behavior of waveguides with multidielectric coatings.**

***Index Terms*—Multilayer, optical reflection, optical waveguides, waveguide discontinuities.**

I. Introduction

MULTILAYER thin film filters are a key technology for low-cost WDM components. The extreme refractive index differences that can be achieved with multilayer thin films enable high-resolution wavelength filters that are orders of magnitude more compact than competing technologies such as fiber Bragg gratings (FBGs). Thin film filters also offer advantages in mass manufacture, where numerous devices can be coated in parallel. This gives thin film filters a significant cost advantage that has seen the majority of large-scale filter manufacturers adopt this technology for production.

FBGs are generally fabricated longitudinally along a waveguide. The fact that the optical field is guided throughout the filter enables extremely long filters that can provide high resolution and also sophisticated functionality. A disadvantage of thin films when compared with FBGs is that they do not provide a guided wave medium while filtering. Thus, once an optical field enters the filter, it will diverge, causing excess losses and other nonideal characteristics. This limits the thickness of filter that can be effectively implemented.

Numerical optimization is a critical component of thin film design as it is difficult for analytic techniques to accommodate material dispersion and other nonidealities. Many tools exist for the simulation and optimization of thin-film filters [1], [2]. These tools generally approximate the optical field as a plane wave (TMM method) [3]. This is only accurate if the filter is short and the divergence angle of the guided mode is small.

Manuscript received April 4, 2005; revised August 29, 2005.

The authors are with the School of Electrical and Computer Engineering, Royal Melbourne Institute of Technology (RMIT), Melbourne, Vic. 3001, Australia (e-mail: s9510300@rmit.edu.au; arnan.mitchell@rmit.edu.au).

Digital Object Identifier 10.1109/JLT.2005.860158

For strongly confined waveguides such as semiconductor waveguides [4], high-index contrast passive waveguides [5], and air clad "photonic wires" [6], the divergence angle will be significant. Further, if very high resolution multifunctional filters are to be realized, significant filter thicknesses may be required. For these cases, the diverging nature of the optical field cannot be ignored. The integration of tightly confined waveguides and sophisticated thin-film filters will be an essential technology for the development of extremely compact photonic components.

Numerical modeling of the propagation of diverging optical fields through thin film structures has been reported using finite difference time domain (FD-TD) [7]–[10], the finite element (FEM) method [11], and bidirectional beam propagation methods (BPM) that require many iterations [12], [13] or Padé approximations to the square-root operator [14]–[17]. These techniques produce accurate results but can be computationally intensive. For practical optimization, it is essential that the model is highly efficient with individual simulations requiring only a few seconds at most. The fact that multilayer thin films are homogeneous in two dimensions offers an opportunity to significantly simplify the modeling of optical propagation within thin films without sacrificing accuracy.

Rigorous analysis of multilayer coated normal facets has been proposed by Vassallo [18] using an integral equation technique and by Smartt *et al.* [19] based on Fourier operators. These methods provide exact results, but their complexity may preclude their applications in numerical optimization design flow.

The plane wave expansion method has been applied in the analysis of coated waveguides, where the field in the waveguide is considered to be the summation of plane waves. Models using several different approximations to the refractive index of the medium that the plane waves see in the waveguide region have been reported. In [20], the plane waves were assumed to travel in homogeneous media whose refractive indices are equal to the refractive index of the core or cladding. This approach cannot be applied to waveguides with a continuous change of refractive index such as diffused waveguides.

In another approach, the effective index of the guided mode has been used as the refractive index of the homogeneous medium [21]. However, this assumption is only valid if the waveguide is weakly guided. A better approach was proposed by Vassallo [18], [22], [23] by replacing the waveguide with a homogeneous medium of equivalent refractive index, which is again only valid for waveguides with little refractive index variation.

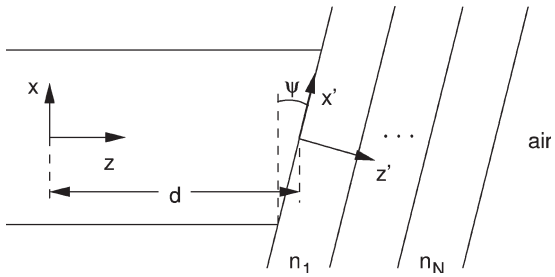

Fig. 1. Configuration of multilayer dielectric coated waveguide.

To minimize the errors incurred by homogeneous medium assumptions, the free-space radiation modes (FSRM) method was proposed [24]–[26]. In this method, the radiation modes in the reflected field were considered and assumed to propagate in a region of uniform refractive index equal to the effective index of the incident guided mode. The FSRM only applies to dielectric waveguides whose refractive index profile is of low contrast [24].

Still using the plane wave expansion method but the homogeneous medium assumption was removed in [27]. That approach can be applied to any waveguide structure. However, only closed-form analysis of integrated mirrors of slab waveguide was considered in [27].

In this paper, that approach is explored further to the analysis of multilayer dielectric coatings on waveguides with normal and angled facets. It is shown that the method not only accurately models the nonplanar propagation characteristics of optical modes but also is extremely efficient. Further, the use of plane wave expansion can also provide insight and understanding of the complex interaction between guided modes and unguided multilayer films.

Section II reviews the plane wave expansion model and the plane wave reflection on a multilayer stack. Section III presents the results and discussions of the analysis of antireflection and high-reflection coatings. The accuracy of the simulations is verified by comparing with other modeling methods. Finally, Section IV will conclude this paper.

II. Theory

The following sections review the plane wave expansion method [18], [20]–[23], [27] and develop theory for its application to the rigorous modeling of multilayer thin film coatings.

A. Plane Wave Expansion

A two-dimensional (2-D) waveguide whose facet is coated with alternating low and high index material as shown in Fig. 1 is considered. The waveguide is assumed to be longitudinally invariant and the incident field is assumed to be transverse in the y-direction and propagate in the z-direction. The dielectric layers are assumed to be parallel, infinite in extent, and perfectly smooth. It is also assumed that the mode shapes of the waveguide-guided modes are not altered by the termination.

The guided incident electromagnetic field in the waveguide is expressed as

$$\varepsilon_g(x,z) = u_g(x)e^{-jk_g z} \tag{1}$$

where $u_g(x)$ is the guided mode profile of the waveguide, and k_g is the propagation constant of that mode. $\varepsilon_g = E_y$ for TE mode, and $\varepsilon_g = H_y$ for TM mode.

At the input plane $z = 0$, the field can be considered as a superposition of an infinite number of elementary plane waves with different wave vectors [21], [27], i.e.,

$$u_g(x) = \int_{-\infty}^{\infty} \widetilde{u}_g(k_x)e^{-jk_x x}\,dk_x \tag{2}$$

where k_x is the propagation constant along the x-axis of each plane wave, the z-component of the propagation constant is $k_z = k_g$, and $\widetilde{u}_g(k_x)$ is the complex spectral amplitude of each plane wave. $\widetilde{u}_g(k_x)$ can be found by the inverse Fourier transform with spatial frequency k_x, i.e.,

$$\widetilde{u}_g(k_x) = \int_{-\infty}^{\infty} u_g(x)e^{jk_x x}\,dx. \tag{3}$$

As it has been assumed that each layer is homogeneous, to accurately simulate the guiding structure at the input, each elementary plane wave is modeled as travelling in an equivalent medium whose refractive index is given by [27]

$$n(k_x) = \sqrt{\frac{k_x^2 + k_z^2}{k_0^2}} \tag{4}$$

where k_0 is the propagation constant of the plane wave in free space, and with propagation angle $\varphi(k_x) = \tan^{-1}(k_x/k_z)$. As each plane wave is associated with its own equivalent medium, this approach overcomes homogeneous medium assumptions of [21] and [23].

At distance z from the origin, the incident field is

$$\varepsilon_g(x,z) = \int_{-\infty}^{\infty} \widetilde{u}_g(k_x)e^{-jk_x x}e^{-jk_g z}\,dk_x. \tag{5}$$

On the surface of waveguide facet, the incident field can be expressed in (x', z') coordinate system as

$$\varepsilon_g(x',0) = \int_{-\infty}^{\infty} \widetilde{u}_g(k_x)e^{-jk'_x x' - j\phi}\,dk_x \tag{6}$$

where

$$k'_x = k_x\cos\psi - k_g\sin\psi \tag{7a}$$

$$\phi = k_g d. \tag{7b}$$

In the waveguide section, each elementary plane wave associated with k_x is modeled as travelling in a homogeneous medium of refractive index $n(k_x)$, and when it is incident on the multilayer dielectric stack at an angle $\theta(k_x) = \varphi(k_x) + \psi$, it will be reflected back into the waveguide region with the reflection coefficient $r(k_x)$ that can be found by the recursive matrix equation as described in Section II-B. By combining

all the reflected plane waves, the total reflected field from the waveguide/coating interface can be found as

$$\varepsilon_r(x') = \int_{-\infty}^{\infty} \widetilde{u}_g(k_x) r(k_x) e^{-jk'_x x' - j\phi}\, dk_x. \tag{8}$$

Converting to (x, z) coordinate system, the reflected field is expressed as

$$\varepsilon_r(x) = \int_{-\infty}^{\infty} \widetilde{u}_g(k_x) r(k_x) e^{-jk_{x_r} x - j\phi}\, dk_x \tag{9}$$

where

$$k_{x_r} = -k_x \cos(2\psi) - k_g \sin(2\psi). \tag{10}$$

Rewriting (9) in terms of k_x, we have the reflected field

$$\varepsilon_r(x) = e^{-j\phi} e^{jk_g \sin(2\psi)x} \int_{-\infty}^{\infty} \widetilde{u}_g(k_x) r(k_x) e^{jk_x \cos(2\psi)x}\, dk_x. \tag{11}$$

It can be seen from (11) that the reflected field can be quickly found by the inverse Fourier transform of $\widetilde{u}_g(k_x) r(k_x)$.

The reflected field can be coupled into all of the different orthogonal guided modes and radiation modes that are supported by the waveguide. It is our main interest here to look at the power that is reflected back into the incident mode. The power reflectivity can be found as the overlap integral between the reflected field and the field profile of the incident mode

$$R = \left(\frac{\left| \int_{-\infty}^{\infty} \varepsilon_r(x) u_g^*(x)\, dx \right|}{\int_{-\infty}^{\infty} |u_g(x)|^2\, dx} \right)^2 \tag{12}$$

for TE mode, and

$$R = \left(\frac{\left| \int_{-\infty}^{\infty} n^{-2}(x) \varepsilon_r(x) u_g^*(x)\, dx \right|}{\int_{-\infty}^{\infty} |n^{-2}(x) u_g(x)|^2\, dx} \right)^2 \tag{13}$$

for TM mode, where $u_g^*(x)$ represents the complex conjugate of the incident mode field profile, and $n(x)$ is the index profile of the waveguide.

The plane wave expansion model described above can be applied to waveguide structures of arbitrary index profile and any guided mode. The guided mode field distribution and the mode propagation constant can be found using any simulation tool including closed form and numerical techniques. In this paper, all Fourier transform calculations were done by fast Fourier transform (FFT) using FFTW library [28].

B. Plane Wave Reflection on Multilayer Dielectric

For the plane wave incident from the medium of index n_0 with the incident angle θ_0 on the stack of N dielectric layers followed by a semi-infinite region of index n_{N+1} that is usually air, we have the following relationship between the fields at the input and output media, i.e.,

$$\begin{bmatrix} u_0^+ \\ u_0^- \end{bmatrix} = \mathbf{R}_{0,1}\mathbf{P}_1 \ldots \mathbf{P}_N \mathbf{R}_{N,N+1} \begin{bmatrix} u_{N+1}^+ \\ u_{N+1}^- \end{bmatrix} = \mathbf{M} \begin{bmatrix} u_{N+1}^+ \\ u_{N+1}^- \end{bmatrix} \tag{14}$$

where n_0^+ and n_0^- are the incident field and reflected field in region n_0, u_{N+1}^+ and u_{N+1}^- are the transmitted field and incident field in region n_{N+1}, $\mathbf{R}_{i,i+1}$ is the transfer matrix on the interface between layer i and layer $i+1$, and $\mathbf{P}_i$ is the propagation matrix in layer i. The transfer matrix and propagation matrix are given as

$$\mathbf{R}_{i,i+1} = \frac{1}{T_{i,i+1}} \begin{bmatrix} 1 & \Gamma_{i,i+1} \\ \Gamma_{i,i+1} & 1 \end{bmatrix} \tag{15}$$

and

$$\mathbf{P}_i = \begin{bmatrix} e^{jn_i k_0 t_i \cos\theta_i} & 0 \\ 0 & e^{-jn_i k_0 t_i \cos\theta_i} \end{bmatrix} \tag{16}$$

where θ_i is the propagation angle of the plane wave in layer i, t_i is the layer thickness, and $\Gamma_{i,i+1}$ and $T_{i,i+1}$ are the Fresnel reflection coefficient and transmission coefficient between layer i and $i+1$, which are given as

$$T_{i,i+1} = \frac{2n_i \cos\theta_i}{n_i \cos\theta_{i+1} + n_{i+1} \cos\theta_i} \tag{17a}$$

$$\Gamma_{i,i+1} = \frac{n_{i+1} \cos\theta_i - n_i \cos\theta_{i+1}}{n_i \cos\theta_{i+1} + n_{i+1} \cos\theta_i} \tag{17b}$$

for TM mode, and

$$T_{i,i+1} = \frac{2n_i \cos\theta_i}{n_i \cos\theta_i + n_{i+1} \cos\theta_{i+1}} \tag{18a}$$

$$\Gamma_{i,i+1} = \frac{n_i \cos\theta_i - n_{i+1} \cos\theta_{i+1}}{n_i \cos\theta_i + n_{i+1} \cos\theta_{i+1}} \tag{18b}$$

for TE mode.

As there is no field input at the far side of the multilayer thin film, we have the boundary condition $u_{N+1}^- = 0$. It is possible to arbitrarily choose the value of u_{N+1}^+, and thus, matrix (14) can be solved. The plane wave reflection coefficient is calculated as

$$r = \frac{u_0^-}{u_0^+} = \frac{m_{21}}{m_{11}} \tag{19}$$

where m_{21} and m_{11} are the elements of the matrix $\mathbf{M}$ in (14).

III. Results and Discussion

In this section, the simulation method described in Section II will be applied to the analysis of multilayer dielectric coatings on optical waveguide facets. Although the described method is suitable for any waveguide structure, for the simplicity of comparison with published results, only symmetric slab waveguide structures will be considered in the following analysis.

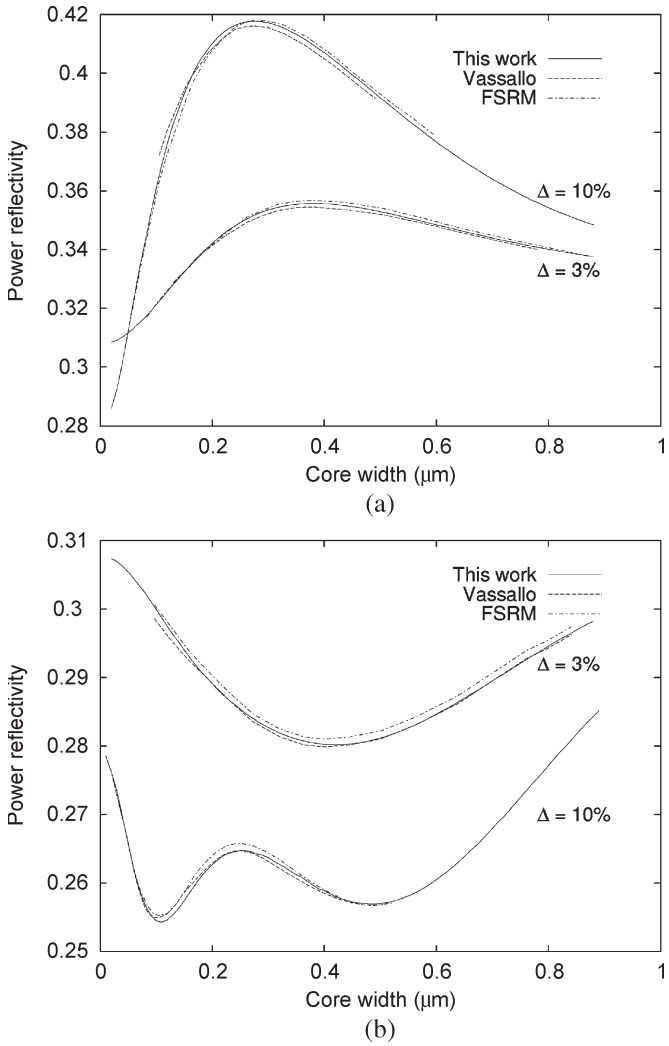

Fig. 2. Power reflectivity as a function of waveguide core width at various variations of cladding index. (a) TE mode. (b) TM mode.

First, the accuracy of the method is verified by comparing with the exact benchmark results of Vassallo [18] for the simple case of normal interface of waveguide with air. The waveguide has a core refractive index $n_{co} = 3.6$ and a cladding index $n_{cl} = 3.6(1 - \Delta)$. The operational wavelength is 0.86 μm. Fig. 2 shows the power reflectivity as a function of the waveguide core width with different cladding index variations for both fundamental TE and TM modes. Excellent agreement with the exact results of Vassallo [18] is achieved over the whole range. Also displayed in Fig. 2 are the data obtained from the FSRM simulation [24], [25].

The model is now applied to the simulation and analysis of more complex structures. Both antireflection and high reflection multilayer dielectric coatings will be considered.

A. Plane Wave Expansion Modeling of Antireflection Coatings

The plane wave expansion method is now applied to the analysis of antireflection dielectric coatings. The first structure to be considered is a single-layer AR coating at normal incident as in [9]. The core and cladding refractive indices are 3.6 and 3.564, respectively. The waveguide core width is 1.457 μm. The coating index is 1.8938, which is equal to $\sqrt{N_{\text{eff}}}$, where N_{eff} is the effective index of the guided mode at 1.55-μm wavelength. The power reflectivity as a function of coating thickness for the fundamental TE mode is calculated at a fixed wavelength of 1.55 μm. The results are displayed in Fig. 3. The data obtained from FD-TD with perfectly matched layer (PML) absorption boundary condition [9] are shown in the same figure for comparison. It can be seen that the results obtained by both methods are in excellent agreement. The results obtained from the TMM simulation are also shown in Fig. 3. Clearly, there is deviation between results given by the TMM and the other two methods. The TMM method fails to predict the optimal coating thickness.

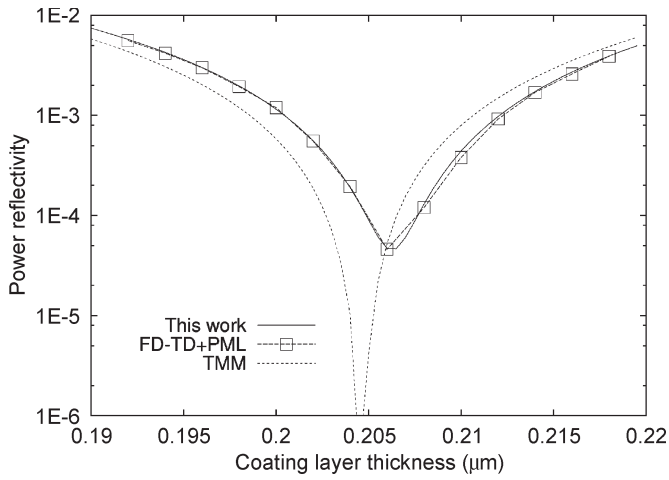

Fig. 3. Power reflectivity of single-layer antireflection coating as a function of coating layer thickness.

It can be seen from Fig. 3 that the TMM method predicts the optimal coating thickness to be a quarter of wavelength $\lambda_g/4 = 0.2046$ μm. Because the TMM method assumes that the waveguide is a homogeneous medium whose refractive index is equal to the effective index of the guided mode, the "impedance match" condition occurs when the coating layer thickness is $\lambda_g/4$. Thus, the reflectivity becomes zero at that coating thickness. However, both the plane wave expansion and FD-TD simulations show that power reflectivity is minimized when the coating thickness is approximately 0.206 μm, which is higher than $\lambda_g/4$. In [9], the optimal coating thickness was observed without any explanation. Here, with the help of plane wave expansion analysis, we can see why the optimal coating thickness is greater than $\lambda_g/4$.

Fig. 4 shows how the reflectivity of fundamental plane waves in the plane wave expansion of the guided mode varies with the coating layer thickness. The inset in Fig. 4 shows the spectral amplitude function $\widetilde{u}_g(k_x)$ of the plane wave expansion. The plane wave corresponding to $k_x = 0$ travels in the equivalent medium that has refractive index equal to the effective index of the guided mode and normal to the waveguide/coating interface. Therefore, the reflectivity for that plane wave is zero at $\lambda_g/4$ coating thickness. For other fundamental plane waves, their equivalent medium refractive indices are higher than the effective index of the guided mode, and their incident angles

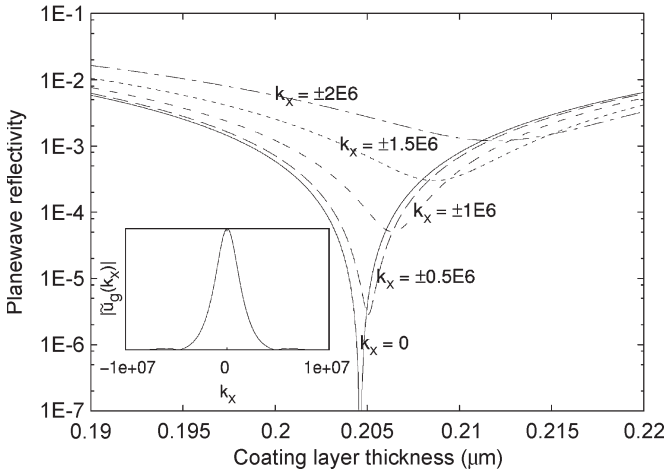

Fig. 4. Reflectivity of the fundamental plane waves as a function of coating layer thickness.

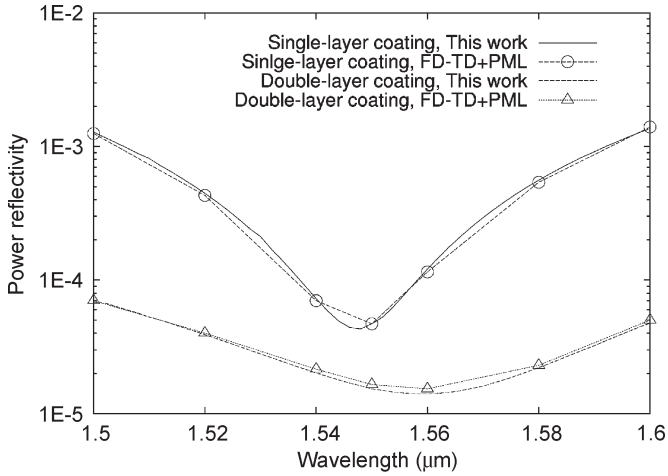

Fig. 6. Power reflectivity as a function of wavelength for antireflection coatings.

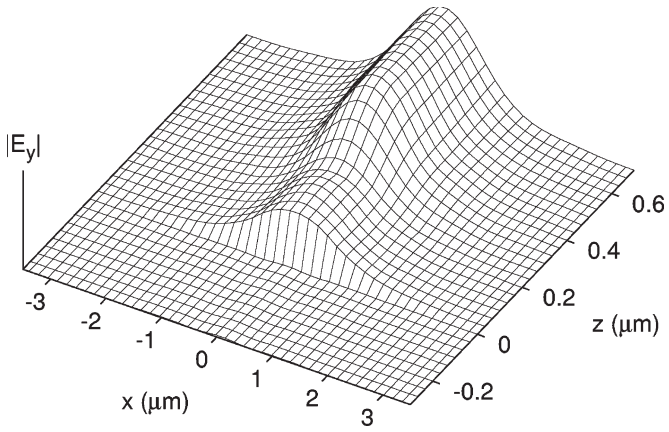

Fig. 5. Field distribution of single-layer antireflection coating.

are nonzero. These angled plane waves have damped reflection resonances at thicknesses greater than $\lambda_g/4$. The total reflected power is the sum of all of these reflectance responses and thus the net effect is a shifted resonance with a damped null.

Fig. 5 shows the steady field distribution of the single-layer AR coating with a coating thickness of 0.206 μm and a wavelength of 1.55 μm obtained using the plane wave expansion simulation. The coating layer is placed at the position $z = 0.2$ μm. All field components (including transmitted and reflected fields) are plotted in the region $z > 0$. In the waveguide section $0 < z < 0.2$ μm, there is little disturbance to the field profile of the guided mode. In the region $z \leq 0$, only the reflected field is plotted. The field in this region is almost zero. These observations illustrate that the reflected field is successfully suppressed by the coating layer.

Next, we consider the power reflectivity of AR coatings as a function of wavelength. In Fig. 6, the power reflectivity at different wavelengths for single-layer coating and double-layer coating at normal incident obtained from both plane wave expansion and FD-TD [9] methods is shown. The single-layer coating thickness is fixed at 0.206 μm. For the double-layer coating, the first layer has an index of 2.76494 and a thickness of 0.138 μm, and the second layer has an index of 1.46 and a thickness of 0.266 μm. Again, the plane wave expansion method gives excellent agreement with the FD-TD method. It is obvious that the double-layer coating gives lower reflectivity at broader band than the single-layer coating.

The effect of waveguide end-face tilt angle on the power reflectivity of single-layer AR coating when the layer thickness is 0.206 μm is shown in Fig. 7(a). It can be seen that the combination of dielectric coating and correct facet angle can achieve near zero reflectivity. The power reflectivity as a function of facet angle calculated by FD $-$ TD $+$ PML [29] is also displayed in Fig. 7(a). The two methods agree well when the angle is small. However, differences between results emerge as the angle increases. In the plane wave expansion model, the modal distribution is assumed to be unaffected by the termination structure of coating layers. This assumption may not be valid when the facet angle is large. At large facet angle, the FD-TD simulation involves staircase approximation of the straight lines of the coating layer interface. Therefore, errors introduced by the staircase approximation become significant when the angle is large and the reflection is very small, unless the grid size used in the FD-TD simulation is very small.

To eliminate the staircase approximation of the FD-TD method, the results given by plane wave expansion modeling are also compared with the FEM $+$ PML simulation with compressed mesh [30]. The FEM method, like the FD-TD approach, also solves Maxwell's equations fully, but uses triangles for discretization, enabling more accurate geometric representation of the angled facet. Although there is a small difference in the reflectivity at large facet angle, the trends of the effects of the facet angle on the reflectivity are similar in the two simulation methods. A further comparison is made with the data obtained from FSRM simulations [31]. It is worthwhile to note that the FSRM method may suffer from the uncertainness of the mode shape assumption as the plane wave expansion method does. All three methods (plane wave expansion, FEM, and FSRM) suggest the same optimal facet angle for antireflection coatings.

The effects of errors due to the staircase approximation in FD-TD simulations are negligible if the reflection is sufficiently large. This is the case of angled facet waveguide without AR

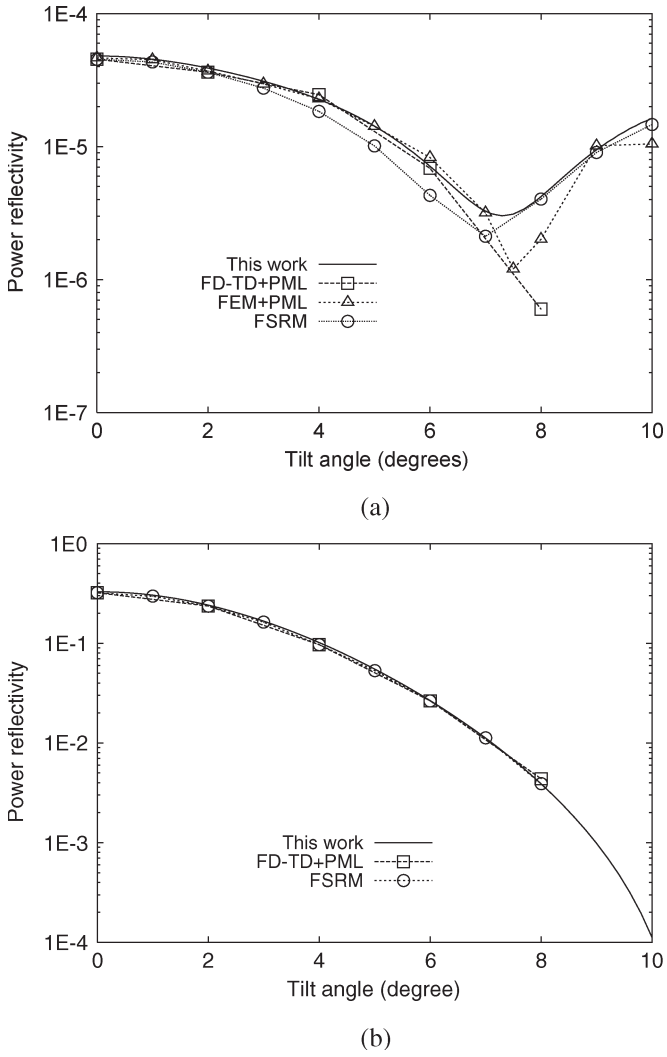

Fig. 7. Power reflectivity as a function of facet angle for antireflection coating. (a) With single layer AR coating of 0.206 μm. (b) Without AR coating.

coating as shown in Fig. 7(b). Data obtained from simulations using plane wave expansion, FD $-$ TD $+$ PML [29], and FSRM [31] methods are presented. Excellent agreement is achieved in this case.

B. Plane Wave Expansion Modeling of High-Reflection Coatings

In this section, the plane wave expansion method is applied to the simulation of high-reflection multilayer dielectric coatings. The waveguide structure used in this analysis is the same as the one in [10]. It has core width of 0.487 μm, cladding refractive index of 3.24, and core refractive index of 3.6. Six layers of quarter-wavelength thickness of two different materials are coated on the end-face. The refractive indices of high and low index materials are 3.5 and 1.7, respectively. Normal incident is assumed.

The wavelength dependency of the power reflectivity for both fundamental TE and TM modes is illustrated in Fig. 8. Throughout the wide range of wavelength, excellent agreement between the simulation by the plane wave expansion method

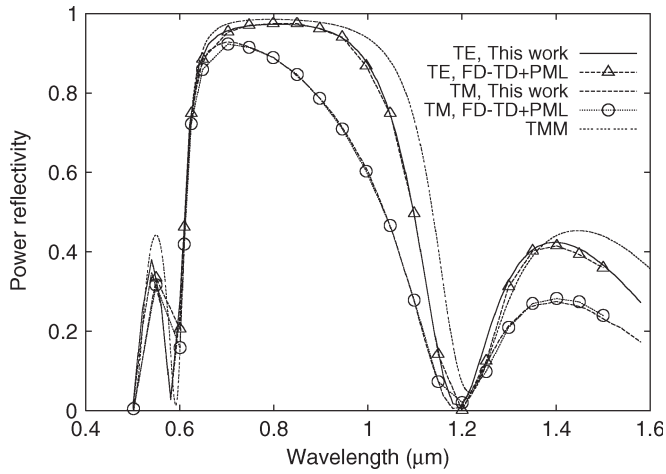

Fig. 8. Reflectivity of high-reflection coating [10] as a function of wavelength.

and the FD-TD with PML data from [10] for both polarizations is achieved. It is clear that the power reflectivity is different for two polarization cases. Shown in Fig. 8 is the power reflectivity calculated by the TMM method when the waveguide region is assumed to be a homogeneous region whose refractive index is equal to the effective index of the guided mode. Obviously, the TMM method fails to predict correctly the reflectivity of high-reflection coatings, especially for TM mode.

Fig. 9(a) and (b) shows the guided mode and reflected field profile for fundamental TE and TM modes, respectively. The data were calculated at a wavelength of 0.8 μm. There are attenuation in the amplitude of the reflected field and mode mismatch between the reflected field and the guided mode. The comparison of Fig. 9(a) and (b) reveals that the reflected field of the TM mode has a lower amplitude than the TE mode. The reflected field profile of the TM mode tends to be much broader than that of the TE mode. These observations can explain why the TM mode has a lower power reflectivity as compared with the TE mode.

C. Plane Wave Expansion Analysis of Polarization Dependence of Reflection

In the previous section, a difference in the reflection of TE and TM modes was observed. In this section, we will analyze the impact of polarization on the reflectivity of multilayer coatings. The spectrum of the plane wave expansion will be used as an analytic tool to see the effects of polarizations on the reflected fields.

The plane wave reflectance coefficients as a function of plane wave spectrum for both TE and TM modes are plotted in Fig. 10. The difference in the plane wave reflectance coefficients of TE and TM modes is clearly visible in Fig. 10. Over the whole plane wave spectrum range, the reflectance coefficients of the TE mode are higher than those of the TM mode. For TM mode, the multilayer coating has a more abrupt response than the TE mode. Therefore, the reflected field of TM mode has a lower amplitude and more mode mismatch as has been illustrated in Fig. 9(a) and (b).

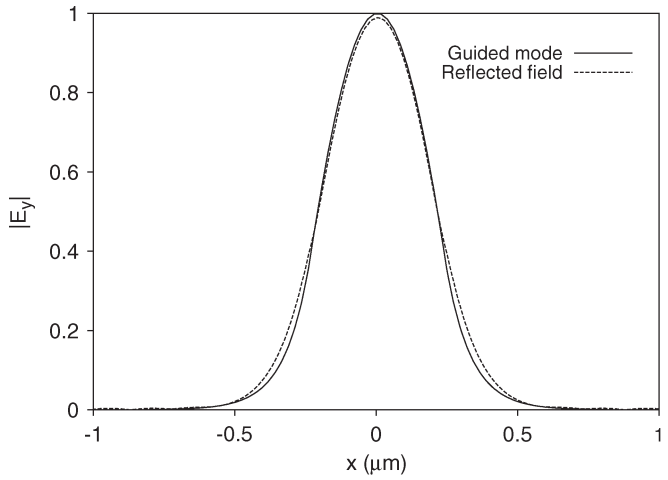

(a)

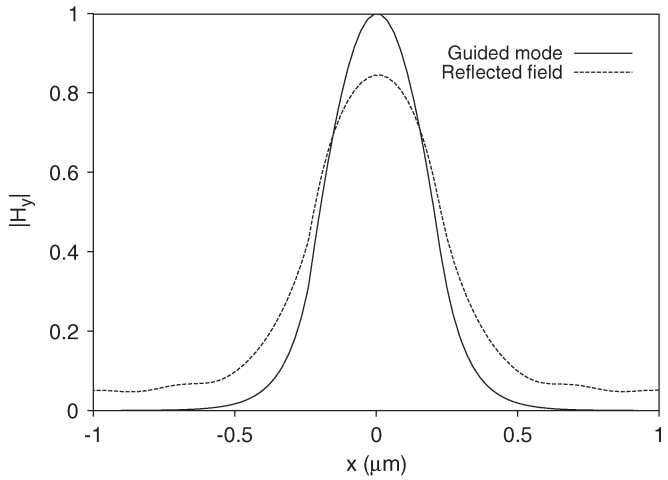

(b)

Fig. 9. Incident guided mode and reflected field profile of (a) TE mode and (b) TM mode of high-reflection coating.

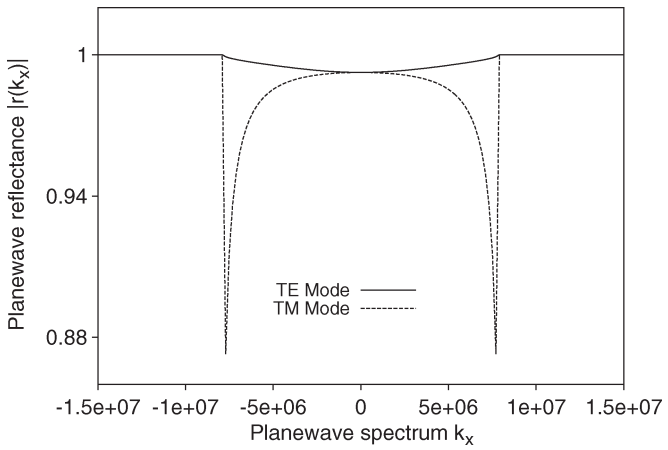

Fig. 10. Plane wave reflectance coefficient as a function of plane wave spectrum of TE and TM modes for high-reflection coatings.

From Fig. 10, it is expected that the reflection of the TM mode will approach that of the TE mode when the plane wave spectral function $\widetilde{u}_g(k_x)$ of the guided mode becomes very narrow or, equivalently, the mode profile is very broad. In the case where $\widetilde{u}_g(k_x)$ is a delta function, the power reflectivity of TE and TM modes is equal to the results given by the TMM method. That condition only happens when the waveguide is a homogeneous medium, and it is consistent with the assumption of the TMM method.

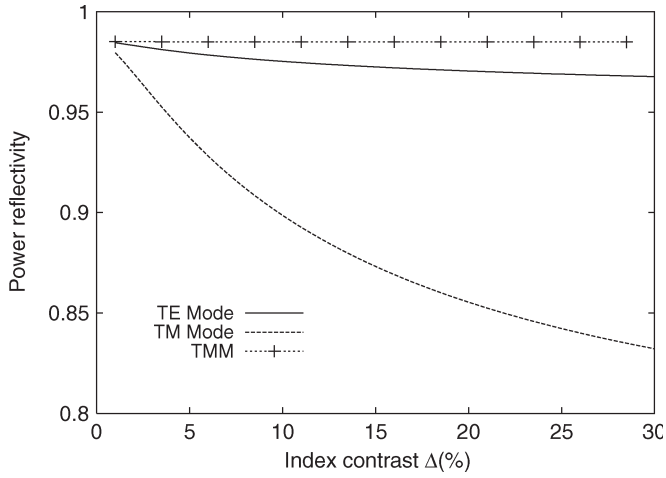

Fig. 11. Power reflectivity as a function of waveguide index contrast.

To illustrate the effects of mode shapes on the reflection as discussed above, the effects of index contrast between the core and the cladding of the waveguide to the power reflectivity are considered. By keeping the core index constant at 3.6 and varying the cladding index as $n_{cl} = (1 - \Delta)n_{co}$, the power reflectivities for both TE and TM modes were calculated and are shown in Fig. 11. When the index contrast is small, the mode is weakly guided. As expected, the power reflectivity for both polarizations approach the value calculated by the TMM method. The guided mode profile is well confined or the plane wave spectral function is broader when the index contrast is increased. Therefore, the difference in the reflection between TE mode, TM mode, and the results obtained by the TMM is larger with a higher index contrast. From these observations, it can be seen that the TMM method can provide satisfactory results only when the waveguide mode is very weakly guided.

IV. Conclusion

In this paper, we have successfully applied the plane wave expansion method to the analysis of multilayer dielectric coatings on optical waveguide facets. The analysis has been carried out for both antireflection and high-reflection coatings. It is shown that the plane wave expansion method is capable of handling the small power reflectivity of antireflection coatings as well as high power reflection cases. To assess the accuracy of the method, the results obtained from the plane wave expansion method were compared with data from exact modeling and other simulation tools. The plane wave expansion method gives excellent agreement results to other simulation methods. Furthermore, the described method has also been used as an analytic tool to provide insight into the understanding of the behavior of the waveguides with multilayer dielectric

coatings, which cannot be easily achieved with other numerical methods.

In comparison with other numerical methods for analyzing multilayer dielectric coatings, the plane wave expansion method gives great advantage in terms of efficiency. On a Pentium IV 2-GHz system, it takes less than 70 ms for each run for a six-layer stack with 512-point FFT. The effect of the number of stack layers on the runtime is minimal, whereas the FD-TD and FEM methods usually take at least several minutes and in some cases may hours to run. Thus, the plane wave expansion method discussed in this paper is very suitable for direct numerical optimization [32].

REFERENCES

[1] *Macleod Optical Thin-Film Software*. [Online]. Available: http://www.thinfilmcenter.com

[2] *Filmstar Optical Thin-Film Software*. [Online]. Available: http://www.ftgsoftware.com

[3] H. Macleod, *Thin-Film Optical Filters*, 2nd ed. Bristol, U.K.: Adam Hilger, 1986, ch. 1–4.

[4] T. Lynch, M. MacBean, R. Walling, and A. Thurlow, "Design and fabrication of packaged PnP/InGaAsP multiple quantum well waveguide components with very low insertion loss," *Proc. Inst. Elect. Eng.—Optoelectron.*, vol. 138, no. 5, pp. 319–322, Oct. 1991.

[5] A. Sakai, G. Hara, and T. Baba, "Propagation characteristics of ultrahigh-Δ optical waveguide on silicon-on-insulator," *Jpn. J. Appl. Phys.*, vol. 40, no. 4B, pp. L383–L385, 2001.

[6] J. Knight, T. Birk, P. Russell, and D. Atkin, "All-silica single-mode optical fiber with photonic crystal cladding," *Opt. Lett.*, vol. 21, no. 19, pp. 1547–1549, Oct. 1996.

[7] S.-T. Chu and S. Chaudhuri, "A finite-difference time-domain method for the design and analysis of guided-wave optical structures," *J. Lightw. Technol.*, vol. 7, no. 12, pp. 2033–2038, Dec. 1989.

[8] W. Huang, S. Chu, A. Goss, and S. Chaudhuri, "A scalar finite-difference time-domain approach to guided-wave optics," *IEEE Photon. Technol. Lett.*, vol. 3, no. 6, pp. 524–526, Jun. 1991.

[9] J. Yamauchi, M. Mita, S. Aoki, and H. Nakano, "Analysis of antireflection coatings using the FD-TD method with the PML absorbing boundary condition," *IEEE Photon. Technol. Lett.*, vol. 8, no. 2, pp. 239–241, Feb. 1996.

[10] J. Yamauchi, H. Kanbara, and H. Nakano, "Analysis of optical waveguides with high-reflection coatings using the FD-TD method," *IEEE Photon. Technol. Lett.*, vol. 10, no. 1, pp. 111–113, Jan. 1998.

[11] S. Wiechmann, H. Heider, and J. Muller, "Analysis and design of integrated optical mirrors in planar waveguide technology," *J. Lightw. Technol.*, vol. 21, no. 6, pp. 1584–1591, Jun. 2003.

[12] P. Kaczmarski and P. Lagasse, "Bidirectional beam propagation method," *Electron. Lett.*, vol. 24, no. 11, pp. 675–676, May 1988.

[13] H. Rao, R. Scarmozzino, and R. M. Osgood, Jr., "A bidirectional beam propagation method for multiple dielectric interfaces," *IEEE Photon. Technol. Lett.*, vol. 11, no. 7, pp. 830–832, Jul. 1999.

[14] H. El-Refaei, I. Betty, and D. Yevick, "The application of complex Pade approximants to reflection at optical waveguide facets," *IEEE Photon. Technol. Lett.*, vol. 12, no. 2, pp. 158–160, Feb. 2000.

[15] H. El-Refaei, D. Yevick, and I. Betty, "Stable and noniterative bidirectional beam propagation method," *IEEE Photon. Technol. Lett.*, vol. 12, no. 4, pp. 389–391, Apr. 2000.

[16] P. Ho and Y. Lu, "A stable bidirectional propagation method based on scattering operators," *IEEE Photon. Technol. Lett.*, vol. 13, no. 12, pp. 1316–1318, Dec. 2001.

[17] ——, "A bidirectional beam propagation method for periodic waveguides," *IEEE Photon. Technol. Lett.*, vol. 14, no. 3, pp. 325–327, Mar. 2002.

[18] C. Vassallo, "Reflectivity of multidielectric coatings deposited on the end facet of a weakly guiding dielectric slab waveguide," *J. Opt. Soc. Amer. A, Opt. Image Sci.*, vol. 5, no. 11, pp. 1918–1928, Nov. 1988.

[19] C. Smartt, T. Benson, and P. Kendall, "Exact analysis of waveguide discontinuities: Junctions and laser facets," *Electron. Lett.*, vol. 29, no. 15, pp. 1352–1353, Jul. 1993.

[20] T. Saitoh, T. Mukai, and O. Mikami, "Theoretical analysis and fabrication of antireflection coatings on laser-diode facets," *J. Lightw. Technol.*, vol. LT-3, no. 2, pp. 288–293, Apr. 1985.

[21] S. Lau, T. Shiraishi, P. McIsaac, A. Behfar-Rad, and J. Ballantyne, "Reflection and transmission of a dielectric waveguide mirror," *J. Lightw. Technol.*, vol. 10, no. 5, pp. 634–643, May 1992.

[22] C. Vassallo, "Polarisation-independent antireflection coatings for semiconductor optical amplifiers," *Electron. Lett.*, vol. 24, no. 1, pp. 61–62, Jan. 1988.

[23] ——, "Theory and practical calculation of antireflection coatings on semiconductor laser diode optical amplifiers," *Proc. Inst. Elect. Eng.—J (Optoelectron.)*, vol. 137, no. 4, pp. 193–202, Aug. 1990.

[24] P. Kendall, D. Roberts, P. Robson, M. Adams, and M. Robertson, "Semiconductor laser facet reflectivities using free-space radiation modes," *Proc. Inst. Elect. Eng.—J*, vol. 140, no. 1, pp. 49–55, Feb. 1993.

[25] ——, "New formula for semiconductor laser facet reflectivity," *IEEE Photon. Technol. Lett.*, vol. 5, no. 2, pp. 148–150, Feb. 1993.

[26] M. Reed, T. Benson, P. Kendall, and P. Sewell, "Antireflection-coated angled facet design," *Proc. Inst. Elect. Eng.—Optoelectron.*, vol. 143, no. 4, pp. 214–220, Aug. 1996.

[27] R. Orobtchouk, S. Laval, D. Pascal, and A. Koster, "Analysis of integrated optical waveguide mirrors," *J. Lightw. Technol.*, vol. 15, no. 5, pp. 815–820, May 1997.

[28] M. Frigo and S. G. Johnson, "FFTW: An adaptive software architecture for the FFT," in *Proc. IEEE Int. Conf. Acoustics Speech and Signal Processing*, Seattle, WA, 1998, vol. 3, pp. 1381–1384.

[29] J. Yamauchi, S. Aoki, and H. Nakano, "Reflectivity analysis of optical waveguides with coated and tilted facets using the FD-TD method with the PML absorbing boundary condition," in *Conf. Edition. Summaries Papers Presented Topical Meeting, Integrated Photonics Research. Tech. Dig. Series*, Boston, MA, 1996, vol. 6, pp. 422–425.

[30] A. Mitchell, D. Kokotoff, and M. Austin, "Improvement to the PML boundary condition in the FEM using mesh compression," *IEEE Trans. Microw. Theory Tech.*, vol. 50, no. 5, pp. 1297–1302, May 2002.

[31] M. Reed, T. Benson, P. Sewell, and P. Kendell, "The free-space radiation mode method for the analysis of coated angled facets and comparison with a FDTD method," *Microw. Opt. Technol. Lett.*, vol. 15, no. 1, pp. 12–16, 1997.

[32] T. Nguyen and A. Mitchell, "Design of antireflection coatings for CWDM by numerical optimization," in *Proc. Australian Conf. Optical Fiber Technology/Australian Optical Society (ACOFT/AOS) Conf.*, Canberra, Australia, Jul. 2004.

Thach Giang Nguyen was born in Quang Tri, Vietnam, on 1975. He received the B.Eng. degree (with first class honors) in communication engineering from the Royal Melbourne Institute of Technology (RMIT), Melbourne, Australia, in 1998 and is currently working toward the Ph.D. degree in communication engineering at the School of Electrical and Computer Engineering, RMIT University.

From 1999 to 2002, he was a Design Engineer at VITECO, Vietnam Post and Telecom Corporation. His research interests are the investigation of specialized optical modulators and modeling of integrated photonic devices.

Arnan Mitchell (S'97–M'00) was born in Dublin, Ireland, on February 20, 1973. He received the B.Tech. degree (with honors) in optoelectronics from Macquarie University, NSW, Australia, in 1993 and the Ph.D. degree from the Royal Melbourne Institute of Technology (RMIT), Melbourne, Australia, in 1999.

He was an Australian Photonics CRC Research Fellow at RMIT, investigating broadband and specialized integrated optical modulators and radio frequency (RF) photonic components for communications and signal processing applications. He is currently a Senior Lecturer at the School of Electrical and Computer Engineering, RMIT University. He maintains an active interest in the research of numerical methods required for the design of RF photonic integrated devices.